View metadata, citation and similar papers at core.ac.uk
brought to you by CORE
provided by Repositório do LNEG

A time domain analysis of arrays of floating point-absorber wave energy converters including the effect of nonlinear mooring forces

Pedro C. Vicente[1], António F. de O. Falcão[1] and Paulo A.P. Justino[2]

[1]IDMEC,
Instituto Superior Técnico, Technical University of Lisbon,
1049-001 Lisboa, Portugal
E-mail: pedro.cabral.vicente@ist.utl.pt; antonio.falcao@ist.utl.pt

[2] Laboratório Nacional de Energia e Geologia,
1649-038 Lisboa, Portugal
E-mail: paulo.justino@ineti.pt

Abstract

The extensive exploitation of the offshore wave energy resource may require the deployment of dense arrays of point absorbers, the distance between elements being possibly tens of meters. In such cases, it may be more convenient and economical that only elements in the periphery of the array are directly slack-moored to the sea bottom, while the other elements are prevented from drifting and colliding by connections to adjacent elements.

Previous work was done in a base configuration of three floating point absorbers located at the grid points of an equilateral triangular, with a solid weight located at the centre of the triangle, which was extended to more complex equilateral triangular grid arrays. The study was based on frequency domain analysis which requires, not only the power take-off system (PTO) to be linear, but also linear mooring forces, which is quite unrealistic as a model of slack moorings.

In the present paper those restrictions are removed by using a time-domain, rather than a frequency domain, analysis, which allows nonlinear mooring forces to be considered. The mooring cables are approximately modelled as catenary lines in a quasi-static analysis. The results show very different behaviour for the horizontal and vertical motions of the floating converters, namely the possibility of occurrence of low-frequency horizontal oscillations of large amplitude. Even in the case of incident regular waves, such horizontal motions were found to be non-periodic, a behaviour that is typical of nonlinear systems.

Keywords: Arrays, Catenary, Moorings, Point absorbers, Wave energy.

1. Introduction

Free floating devices are a large class of wave energy converters (WECs) for deployment offshore, typically in water depths between 40 and 100m. As in the case of floating oil and gas platforms, such devices are subject to drift forces due to waves, currents and wind, and so they have to be kept on station by moorings (early contributions to the mooring design of wave energy converters can be found in [1,2]). Although similarities can be found with such applications, the mooring design will have some important differences, one of them associated to the fact that, in the case of a wave energy converter, the mooring connections may significantly modify its energy absorption properties by interacting with its oscillations [3].

Among the wide variety of floating wave energy devices, point absorbers have been object of special development effort since the late 1970s. They are oscillating bodies whose horizontal dimensions are small in comparison with the representative wavelength. Examples of devices are the IPS buoy [4], Aquabuoy [5], Wavebob [6] and PowerBuoy [7]. Their rated power ranges typically from tens to hundreds of kW.

The extensive exploitation of the offshore wave energy resource may require the deployment of dense arrays of absorbers, the distance between elements in the array being possibly tens of meters [8].

However, little attention seems to have been devoted in the published literature to the mooring design of free-floating point absorbers in dense arrays. This may be explained by the present stage of development of the technology (focusing on single prototypes) and/or by the restricted availability of such information.

In such cases, it may be more convenient that only elements in the periphery of the array are directly slack-moored to the sea bottom, while the other elements of the array are prevented from drifting and colliding by connections to adjacent elements.

Such a system was studied in [9], with a base configuration of three floating point absorbers located at the grid points of an equilateral triangle, with a solid weight located at the centre (whose function is to pull the floaters towards each other and keep the inter-body moorings lines under tension). This was extended to more complex equilateral triangular grid arrays. In [9], the study was based on frequency domain analysis which requires, not only the power take-off system (PTO) to be linear, but also linear mooring forces, which is quite unrealistic as a model of slack moorings.

In the present paper those restrictions are removed by using a time-domain, rather than a frequency domain, analysis, which allows nonlinear mooring forces to be considered. The mooring cables are approximately modelled as catenary lines in a quasi-static analysis. This means that, in the relationship between mooring forces and body position, dynamic effects (namely cable inertia and viscous drag forces) are ignored but not the cable weight per unit length. The PTO is assumed to be a linear damper activated by the buoy heaving motion.

Most floating oscillating-body wave energy converters that have been proposed and developed so far are in fact two-body systems, in which the PTO is activated by the relative motion between bodies. The assumption of a single-body WEC whose PTO is activated by the heave motion was adopted here to keep the complexity of the theoretical and numerical modelling within manageable limits, while (as claimed in [10]) providing a qualitative measure for comparison between the situations with and without mooring.

Equations for the time domain analysis are presented for an array of three point absorbers, which can then be extended to build up a mathematical model for more complex equilateral triangular grid arrays in which the floaters are located at the grid points of an equilateral triangular grid. Numerical results, for motions and absorbed power, are presented for arrays of three and seven hemispherical buoys, with slack bottom moorings and inter-body connections and a linear power take-off, both for regular and irregular waves. Comparisons are given with the unmoored and independently-moored buoy situations.

Variations in mean surface level due to tides and drifting forces due to currents and wind are ignored. The PTO consists of a linear damper whose force is assumed proportional to the heave velocity. Taking into account the spherical shape of the buoys and assuming the mooring lines and the PTOs to be attached to the centres of the bodies, it follows that the only significant modes of oscillation are heave, surge and sway.

2. Mathematical Model

We consider three identical hemispherical buoys, 1, 2 and 3, in an equiangular triangular configuration, as shown in plan view in Fig. 1. The moorings consists of a slack system of three mooring lines 1, 2 and 3 connecting buoys 1, 2 and 3 to the sea bottom respectively, and three lines 1-4, 2-4 and 3-4 connecting the buoys to a centrally placed weight 4 (a body much denser than water) whose role is to pull the buoys towards the centre of the triangle.

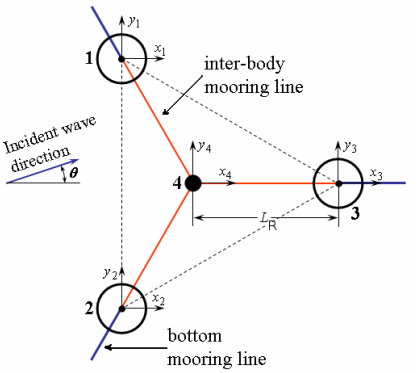

Figure 1: Plan view, in calm-sea static conditions, of the equilateral triangular 3-buoys array. Wave direction makes an angle θ with the x-axes.

All six lines are supposed to be attached to the centres of the bodies. In a plan view and in calm water, the centres of the buoys are located at the vertices of a triangle and the six connecting lines (three bottom-mooring lines and three inter-body mooring lines) are aligned with the bisectors of the triangle (Fig. 1). The direction of propagation of the incident waves makes an angle θ with the x-axes, as shown in Fig. 1.

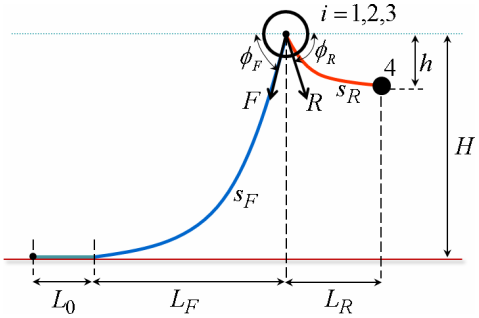

Figure 2: Side view, in calm-sea static conditions, of the mooring arrangement between bottom, buoys and body.

In the absence of waves, we assume that the centres of buoys lie on the free-surface plane, a vertical distance H from the bottom of the sea, and a horizontal distance L_R from the centre of the triangle and a distance $L_R\sqrt{3}$ apart from each other. The buoys are considered to be at an initial horizontal distance $L_0 + L_F$ from the anchor point on the bottom, where L_0 is the length of the cable that initially lays on the seabed and L_F is the horizontal length of the hanging (catenary) part of the cable (see Fig. 2). The centre of body 4 is at distance h below the free surface.

The mooring cables are approximately modelled as catenary lines, are assumed inelastic and their dynamic effects (namely cable inertia and viscous drag forces) are ignored but not the submerged cable weight per unit length W, which depends on the cable material used (like chain, wire, fibre) and its construction ([3]).

The classical catenary equations ([11]) may be written as

$$Z = \left(\frac{T_H}{W}\right)\cosh\left(\frac{D}{T_H/W}+\alpha\right)+\beta, \quad (1)$$

$$s = \left(\frac{T_H}{W}\right)\sinh\left(\frac{D}{T_H/W}+\alpha\right)+\gamma, \quad (2)$$

$$T = T_H\cosh\left(\frac{D}{T_H/W}+\alpha\right), \quad (3)$$

$$T_V = T_H\sinh\left(\frac{D}{T_H/W}+\alpha\right). \quad (4)$$

Here, D and Z are the horizontal and vertical coordinates of the cable point with respect to the lowest point of the catenary (where the cable departs from the bottom); α, β and γ are constants determined from the boundary conditions; s is the length of the catenary-shaped part of the cable; T is the tension force on the cable, and T_H and T_V its horizontal and vertical components; W is the cable weight (minus buoyancy force) per unit length. The tension T_H (the same at every point along the cable) is the main unknown and it (or the ratio T_H/W) is sometimes referred to as the catenary parameter ([3]).

In this scenario, in the initial equilibrium position and for the bottom-mooring cable, we considerer $T=F$, $T_H=F_H$, $T_V=F_V$, $W=W_F$, $\alpha=\alpha_F$, $\beta=\beta_F$, $\gamma=\gamma_F$. The boundary conditions at the point of seabed contact are

$$s=0,\quad D=0,\quad Z=0,\quad dZ/dD=0, \quad (5)$$

which means that the unknown constants in the equations are

$$\alpha_F=0,\quad \beta_F=-F_H/W_F,\quad \gamma_F=0. \quad (6)$$

The boundary conditions at the buoy would then be $D=L_F$ and $Z=H$, which, together with W_F, make possible to calculate the initial horizontal cable tension F_H by resolving the following non-linear equation with an appropriate root-finding algorithm

$$H = \left(\frac{F_H}{W_F}\right)\left[\cosh\left(\frac{L_F}{F_H/W_F}\right)-1\right]. \quad (7)$$

Once the value of F_H is known, it is easy to calculate the remaining parameters such as F_V, F and the hanging cable length s_F. The bottom-mooring cable total length would then be $l_F = s_F + L_0$.

The angle θ_F (with the horizontal plane) of the cable at the buoy attachment point can be easily found by considering

$$\cos\phi_F = F_H/F. \quad (8)$$

Since the horizontal tension force F_H is assumed to be the same at every point of the (bottom-mooring) cable, then, for the static situation (absence of waves), it is also equal to the horizontal tension force in the inter-body mooring cable $R_H = F_H$.

The calculations for the inter-body mooring cable, connecting the buoys and the submerged body 4 (weight) are based on the same catenary equations (1-4), by considering $T=R$, $T_H=R_H$, $T_V=R_V$, $W=W_R$, $\alpha=\alpha_R$, $\beta=\beta_R$, $\gamma=\gamma_R$. We take into account that $R_H = F_H$, that body 4 (weight) is at (horizontal) distance L_R from the buoy and at a depth h (from the undisturbed free surface). We further consider the previous boundary conditions (5) at the buoy. The conditions at body 4 is such that

$$\left.\frac{dZ}{dD}\right|^{+} - \left.\frac{dZ}{dD}\right|^{-} = \frac{P_4}{R_H}, \quad (9)$$

where P_4 is a force downwards (since the body is more dense than water) that is equal to the difference between the body weight and its buoyancy force

$$P_4 = m_4 g - v_4\rho_0 g = v_4(\rho_4-\rho_0)g. \quad (10)$$

For given body density ρ_4, the volume v_4 of body 4 (and consequently body radius a_4) can be determined as functions of L_R and h.

Then it is also possible to calculate the value of $l_R = s_R$, R and R_V and, as before, ϕ_R the angle to the horizontal made by the inter-body cable at the buoy

$$\cos\phi_R = R_H/R. \quad (11)$$

Since, in calm sea, the centres of the hemispherical buoys (of radius a) are supposed to lie on the free-surface plane, the buoy mass m must be

$$m = \frac{2}{3}\pi a^3\rho - \frac{1}{g}(F_V + R_V). \quad (12)$$

This equation expresses that the vertical component of the resultant force on the motionless buoy is zero. Note that, since the buoy centre is assumed to lie on the free-surface horizontal plane in static conditions, the mass m of a moored buoy slightly varies with the mooring parameters, as shown by Eq. (12).

The calculated equilibrium values can be extended to the three buoys, by defining the pulling force vectors F_1, F_2 and F_3 for the bottom-mooring lines, the corresponding angles ϕ_{F1}, ϕ_{F2} and ϕ_{F3}, the tension force vectors R_1 (line 1-4), R_2 (line 2-4) and R_3 (line (3-4), and the corresponding angles ϕ_{R1}, ϕ_{R2} and ϕ_{R3}. In the absence of waves, it is then $F_1=F_2=F_3=F$, $\phi_{F1}=\phi_{F2}=\phi_{F3}=\phi_F$ and $R_1=R_2=R_3=R$, $\phi_{R1}=\phi_{R2}=\phi_{R3}=\phi_R$. Considering the triangular formation, the projections of lines 1-4, 2-4 and 3-4 on the horizontal plane make, with the x-direction, angles $\varphi_1=2\pi/3$, $\varphi_2=-2\pi/3$ and $\varphi_3=0$. In the absence of wave, we have, for $j=1$ to 3,

$$\begin{cases} F_{X,j} = F_H\cos\varphi_j, \\ F_{Y,j} = F_H\sin\varphi_j, \end{cases} \quad (13)$$

for the bottom-moorings, and

$$\begin{cases} R_{X,j} = R_H\cos(\varphi_j+\pi), \\ R_{Y,j} = R_H\sin(\varphi_j+\pi), \end{cases} \quad (14)$$

for the inter-body moorings.

3. Time-domain analysis

The dynamics of floating bodies in waves with nonlinear mooring systems were theoretically studied in connection with moored ships and offshore platforms without wave energy absorption. Analyses can be found of the influence of the mooring lines in the horizontal motion (for e.g. [12]), of the nonlinear dynamics of moored vessels (e.g. [13]). No work on such effects on wave-energy-absorbing floating systems seems to have been published. The nonlinear effects are in general much more significant in the case of slack moorings (with catenary mooring lines, the case analysed here) than for tightly moored floaters. If nonlinearities are to be taken into account, then a time-domain (rather a frequency-domain) analysis is to be employed. This approach was first applied to ships in wavy seas [14] and later extended to oscillating-body energy converters [15].

The buoys and body 4, acted upon by the waves and mooring lines, are made to oscillate in heave and horizontally. The displacements of their centres from their mean positions are defined by coordinates (x_j, y_j, z_j) ($j = 1$ to 4) (x_j and y_j are horizontal coordinates, and z_j is a vertical coordinate pointing upwards) (Fig. 1). In this case, the dynamic equations are, for each buoy $j = 1, 2, 3$,

$$(m + A_{\infty h})\ddot{x}_j(t) + \int_{-\infty}^{t} L_h(t-\tau)\ddot{x}_j(t)d\tau = f_{dh}\cos\theta - F_{X,j}, \quad (15)$$

$$(m + A_{\infty h})\ddot{y}_j(t) + \int_{-\infty}^{t} L_h(t-\tau)\ddot{y}_j(t)d\tau = f_{dh}\sin\theta - F_{Y,j}, \quad (16)$$

$$(m + A_{\infty z})\ddot{z}_j(t) + \rho g S z_j(t) + \int_{-\infty}^{t} L_z(t-\tau)\ddot{z}_j(t)d\tau = f_{dz} - C\dot{z}_j - F_{Z,j} + F_V. \quad (17)$$

Here, $A_{\infty u}$ $(u = h, z)$ are the limiting values of the added masses $A_u(\omega)$ for $\omega = \infty$. For a hemispherical floater, it is $A_{\infty z} = \mu/2$ and $A_{\infty h} = 0.2732\mu$, where $\mu = 2\pi a^3\rho/3$ (see [16]). f_{dh} and f_{dz} are the horizontal (h) and vertical (z) components of the wave excitation force on the buoys (see [17]). The PTO of each floating converter is assumed to consist of a simple linear damper activated by the buoy heaving motion. The vertical force it produces on the buoy is $-C\dot{z}_j$ ($j = 1$ to 3). Finally, $S = \pi a^2$.

The convolution integrals in Eqs. (15-17) represent the memory effect in the radiation forces. Their kernels can be written as

$$L_u(t) = \frac{2}{\pi}\int_{-\infty}^{t} \frac{B_u(\omega)}{\omega}\sin\omega t\, d\omega \quad (u = h, z). \quad (18)$$

They decay rapidly and may be neglected after a few tens of seconds, which means the infinite interval of integration in Eqs. (15-17) may be replaced by a finite one in the numerical calculations (a 20s interval was adopted as sufficient). The integral-differential equations (15-17) were numerically integrated from given initial values of x, z, $\dot{x}$ and $\dot{z}$, with an integration time step of 0.05 s.

$B_u(\omega)$ $(u = h, z)$ are the frequency-dependent hydrodynamic coefficients of radiation damping concerning the horizontal (subscript h) and heave (subscript z) oscillation modes of the spherical buoys.

The time varying values of the bottom-mooring forces $F_{X,j}$, $F_{Y,j}$, $F_{Z,j}$ on each cable, $j = 1$ to 3, are calculated based on the position of each buoy, considering the cable length l_F defined for the static position and the previous catenary equations

$$L_0 + L_F + d_j = (l_F - s_F) + D, \quad (19)$$

$$Z + z_j = \left(\frac{F_{H,j}}{W_F}\right)\cosh\left(\frac{D + d_j}{F_{H,j}/W_F}\right), \quad (20)$$

$$s_F = \left(\frac{F_{H,j}}{W_F}\right)\sinh\left(\frac{D + d_j}{F_{H,j}/W_F}\right). \quad (21)$$

Here d_j is the horizontal displacement from the equilibrium position (with components x_j and y_j). Once $F_{H,j}$ has been calculated, it is easy to calculate also $F_{V,j} = F_{Z,j}$ and F_j, and the values of $F_{X,j}$ and $F_{Y,j}$ for each buoy, by considering the angles between the projection of the mooring lines and the x-direction.

Body 4 is subject to the pulling forces of lines 1-4, 2-4 and 3-4, its own weight, the buoyancy force and the hydrodynamic forces on it. Similar dynamic equations apply

$$(m_4 + A_{\infty 4h})\ddot{x}_4(t) + \int_{-\infty}^{t} L_{4h}(t-\tau)\ddot{x}_4(t)d\tau = f_{d4h}\cos\theta - \sum_{j=1}^{3} R_{4X,j}, \quad (22)$$

$$(m_4 + A_{\infty 4h})\ddot{y}_4(t) + \int_{-\infty}^{t} L_{4h}(t-\tau)\ddot{y}_4(t)d\tau = f_{d4h}\sin\theta - \sum_{j=1}^{3} R_{4Y,j}, \quad (23)$$

$$(m_4 + A_{\infty 4z})\ddot{z}_4(t) + \int_{-\infty}^{t} L_{4z}(t-\tau)\ddot{z}_4(t)d\tau = f_{d4z} - 3R_V + \sum_{j=1}^{3} R_{4Z,j}. \quad (24)$$

The kernels of the convolution integrals L_{4u} $(u = h, z)$ are calculated as before, considering $B_{4u}(\omega)$ $(u = h, z)$ as the hydrodynamic coefficients of radiation damping of body 4. f_{d4h} and f_{d4z} are the horizontal and vertical components of the wave excitation force on body 4. In this case, the effects of the wave radiation and diffraction induced by buoys 1-3 upon body 4 were neglected. For the added mass of body 4, $A_{\infty 4u}$

$(u = h, z)$, we take the added mass of an accelerating sphere in an unbounded fluid (see e.g. [16]) $A_{4h} = A_{4z} = (2/3)\rho\rho\, a_4^3$.

The time varying values of the inter-body mooring forces $R_{4X,j}$, $R_{4Y,j}$, $R_{4Z,j}$ on each cable $j = 1$ to 3 are calculated in a similar way as for the bottom-mooring, considering the boundary conditions and taking into account the values of P_4 and l_R defined for the equilibrium position.

4. Numerical results for a three-buoy array

We set $\rho = 1025\ \mathrm{kg\,m^{-3}}$ (sea water density) and $g = 9.8\ \mathrm{ms^{-2}}$. Body 4 is a sphere of density $\rho_4 = 2500\ \mathrm{kg\,m^{-3}}$ (typical of concrete). The submergence of body 4 is assumed to be sufficient for the excitation force and the radiation damping on it to be neglected, i.e. we set $B_{4h} = B_{4z} = 0$ and $f_{d4h} = f_{d4z} = 0$.

In all cases for which results are shown here, it is, $a = 7.5$ m, $H = 60$ m, $L_0 = 0.65 \times L_F$, $L_F = 60$ m, $L_R = 30$ m, $h = 20$ m and $C = 251.1$ kN/(m/s). A value for the submerged cable weight of $W_F = W_R = 1520$ N/m was used, adequate for example for a 90mm thick chain cable (see [3]). This results in a body of radius $a_4 \approx 0.73$ m, a bottom-mooring cable of length $l_F = 140.75$ m and an inter-body mooring cable of length $l_R = 36.75$ m.

The adopted value of $C = 251.1$ kN/(m/s) is obtained from $C = B$, and is the one that allows maximum wave energy absorption by an isolated unmoored hemispherical heaving buoy, at resonance frequency defined by resonance condition (see e.g. [17])

$$\omega = \left[\frac{m + A(\omega)}{\rho g S}\right]^{-1/2}. \qquad (25)$$

4.1. Regular waves

For regular waves the excitation force components are assumed to be simple-harmonic functions of time and so we may write $\{f_{dx}, f_{dz}\} = \mathrm{Re}\left(\{F_{dx}, F_{dz}\} e^{i\omega t}\right)$, where the complex amplitudes F_{dx} and F_{dz} are proportional to the amplitude A_w of the incident wave. The moduli of F_{dx} and F_{dz} may be written as $\{|F_{dx}|, |F_{dz}|\} = \{\Gamma_x A_w, \Gamma_z A_w\}$, where $\Gamma_x(\omega)$ and $\Gamma_z(\omega)$ are (real positive) excitation force coefficients.

Deep water was assumed for the hydrodynamic coefficients of added mass, radiation damping and excitation force. The frequency dependent numerical values were obtained with the aid of the boundary element code WAMIT, for the radiation damping coefficients $B_u(\omega)$ and the absolute value $\Gamma_u(\omega)$ and phase $\arg\left(F_{dz}(\omega)/F_{dx}(\omega)\right)$ of the excitation forces coefficients, for the floating hemispheres, oscillating horizontally and vertically ($u = h, z$).

The power performance of the three wave energy converters 1, 2 and 3 can be defined by a dimensionless power absorption coefficient defined as $P_j^* = \overline{P}_j / \overline{P}_{\max}$ $(j = 1$ to $3)$, where $\overline{P}_{\max}$ is the theoretical maximum limit of the (time-averaged) power that an axisymmetric heaving wave energy converter can absorb from regular waves of frequency ω and amplitude A_w, and is known to be (see [17]) $\overline{P}_{\max} = g^3 \rho A_w^2 / (4\omega^3)$ (corresponding to capture width $\lambda / 2\pi$).

Numerical results are presented in Figs 3 to 6 for regular waves of $A_w = 1$ m, $T = 10$ s. and $\theta = 0$. Comparisons are shown with buoys of the same size (with identical values of a, H, L_0, L_F, W_F and C as for the triple buoys), individually spread-moored by two cables (in the vertical plane of the incident wave direction) as well as unmoored.

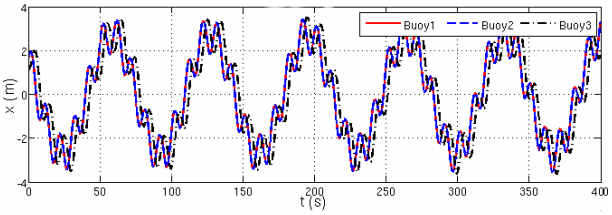

Figure 3: Surge (x) oscillations for individually-moored buoys in regular waves of $A_w = 1$ m, $T = 10$ s.

Fig. 3 shows the surge oscillations for buoys 1 to 3, for the individually-moored buoys. As expected, the time series for buoys 1-2 and buoy 3 are not identical, due to their different locations. Since it is $\theta = 0$, obviously the surge oscillations of buoy 1 and 2 are identical. It may be seen that the surge oscillations exhibit a markedly non-simple-harmonic time-pattern, composed of the wave frequency (0.1 Hz) oscillation superimposed on a low frequency (about 0.018 Hz) oscillation (which can be related to the system natural oscillation frequency), which is obviously a nonlinear effect, not visible, for the same wave conditions, in the frequency-domain analysis [9].

Fig. 4 shows the heave, surge, sway oscillations for buoys 1 to 3, for the inter-body moored array. Like the individually-moored buoys, the non linear surge oscillations are visible and reveal an (even lower) low frequency. The sway oscillations also reveal non linear behaviour (buoys 1 and 2) caused by the angle of the bottom-mooring with the y-direction. The surge and sway oscillations (significantly) exceed those of the heave oscillations and are higher than those predicted by the frequency-domain analysis [9].

Fig. 5 shows the heave z_4, surge x_4 and sway y_4 oscillations for body 4. The surge (and also the heave) oscillation reveal a highly nonlinear behaviour that results from the different nonlinear oscillations of the three buoys to which the body is attached.

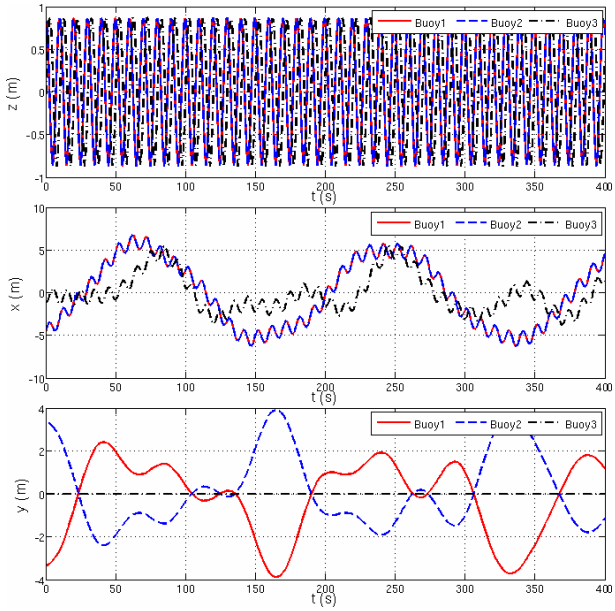

Figure 4: Heave (z), surge (x) and sway (y) oscillations for the inter-body moored buoys in regular waves of $A_w = 1\,\text{m}$, $T = 10\,\text{s}$.

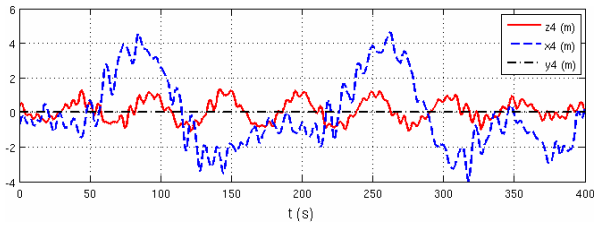

Figure 5: Heave (z_4), surge (x_4) and sway (y_4) oscillations for body 4 in regular waves of $A_w = 1\,\text{m}$, $T = 10\,\text{s}$.

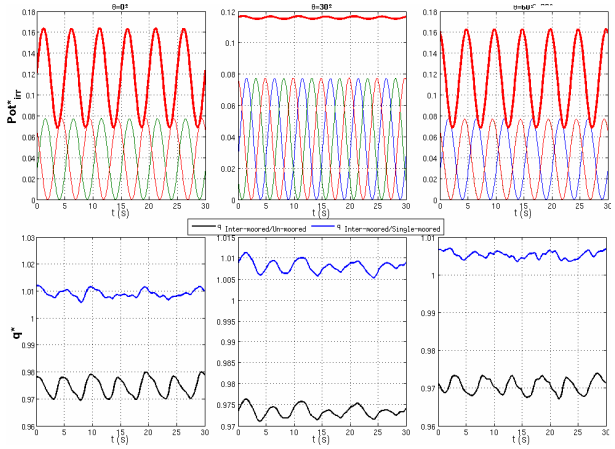

Figure 6: On top: instantaneous dimensionless power absorbed by the three-buoy array with inter-body moorings (red solid line) and by each buoy of the array. Below: ratios between the power absorbed by the triple buoy set and by an identical set in the unmoored and independently moored situations.

Fig. 6 shows, on top, the time-varying power absorbed separately by each buoy, and the total power. As expected, the combination of three converters produces a smoothing effect on power, which would be even more evident in the case of an array with a larger number of elements. The power produced is not significantly affected by the nonlinear oscillations since it is considered that the PTO only extracts power from the heave oscillations. At the bottom, Fig. 6 also shows the ratio between the power absorbed by the triple buoy set and by an identical set in the unmoored and independently moored situations. The inter-body moored configuration appears less favourable than the unmoored configuration ($q^* < 1$), but is slightly better than the individually-moored configuration ($q^* > 1$).

4.2. Irregular waves

Real irregular waves may be represented, in a fairly good approximation, as a superposition of regular waves, by defining a spectrum. Since our wave energy converter is axisymmetric and insensitive to wave direction, it is reasonable to assume the spectrum to be one-dimensional. We adopt the Pierson-Moskowitz spectral distribution, defined by (SI units, [18])

$$S_\zeta(\omega) = 263 H_s^2 T_e^{-4} \omega^{-5} \exp(-1054 T_e^{-4} \omega^{-4}), \quad (26)$$

where H_s is the significant wave height and T_e is the energy period. For linear systems, the time-averaged power output in irregular waves is

$$\overline{P}_{\text{irr}}(H_s, T_e) = 2\int_0^\infty \overline{P}_1(\omega) S_\zeta(\omega)\, d\omega, \quad (27)$$

where $\overline{P}_1(\omega)$ is the power absorbed by the floater from regular waves of frequency ω and unit amplitude. In dimensionless form, we write, for irregular waves, $P^*_{\text{irr}} = \overline{P}_{\text{irr}} / \overline{P}_{\text{max,irr}}$, where

$$\overline{P}_{\text{max,irr}} = \frac{g^3 \rho}{2} \int_0^\infty \omega^{-3} S_\zeta(\omega)\, d\omega = 149.5 H_s^2 T_e^3 \quad (28)$$

(SI units) is the maximum (time-averaged) power that can be extracted by an axisymmetric body oscillating in heave in a sea state represented by the spectral distribution $S_\zeta(\omega)$.

To obtain time-series of the water surface elevation at a point due to irregular waves representative of a particular sea state, various simulation methods can be applied. A commonly used method, assumes that a random Gaussian process can be obtained by the sum of a large number of *N* sinusoidal components with phases randomly generated and deterministic amplitudes derived from the density spectrum.

For time-series calculations, the spectral distribution is then discretized as the sum of a large number N of regular waves of frequency $\omega_n = \omega_0 + n\Delta\omega$, where ω_0 is the lowest frequency considered ($\omega_0/\Delta\omega$ should be an irrational number in order to ensure the non-periodicity in the time-series), $\Delta\omega$ is a small frequency interval, $n = 0, 1, 2, \ldots, N-1$, and the spectrum is supposed not to contain a significant amount of energy outside the frequency range $\omega_0 \le \omega \le \omega_0 + (N-1)\Delta\omega$. The (deterministic) amplitude of the wave component of order n is $A_{wn} = \left(2 S_\zeta(\omega_n)\Delta\omega\right)^{1/2}$.

The excitation force may be written as

$$f_{du}(t) = \sum_n f_{du_n}(t) = \sum_n A_{wn}\, \text{Re}\left\{F_{du}(\omega_n) e^{i(\omega_n t + \phi_n)}\right\} \quad (29)$$

$(u = h, z)$. In the simulations we adopted $\omega_0 = 0.05 + \sqrt{6}$ rad/s, $\Delta\omega = 0.01$ rad/s and $N = 200$. The phase ϕ_n of each component was chosen as a random real number in the interval $(0, 2\pi)$.

Results are plotted in Figs. 7-8, for irregular waves of $H_s = 2$ m, $T_e = 10$ s, $\theta = 0$, for $a = 7.5$ m, $H = 60$ m, $L_0 = 0.65 \times L_F$, $L_F = 60$ m, $L_R = 30$ m, $h = 20$ m, $W_F = W_R = 1520$ N/m and $C = 251.1$ kN/(m/s).

Fig. 7 shows the heave, surge and sway oscillations for buoys 1 to 3 in irregular waves. It can be seen that the system low frequency oscillation in sway and surge are still present and that their amplitude has not significantly changed.

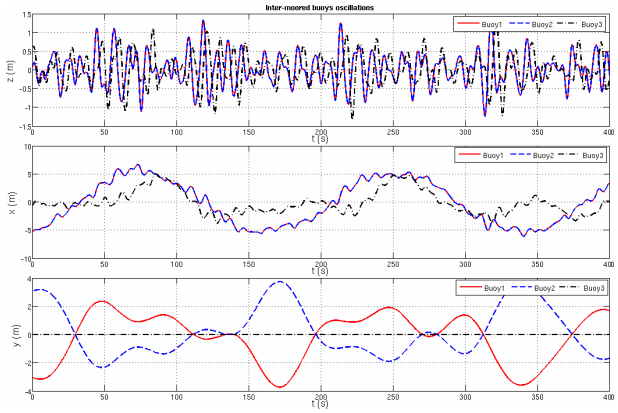

Figure 7: Heave, surge and sway oscillations for the inter-body moored buoys .Irregular waves of $H_s = 2$ m, $T_e = 10$ s.

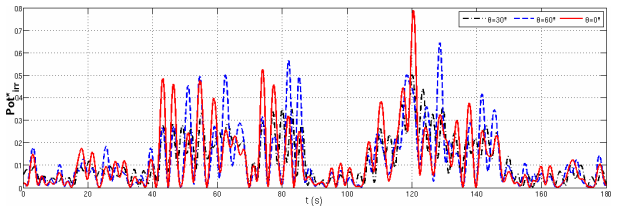

Figure 8: Comparison between the dimensionless power absorbed by the three buoys in array with inter-body moorings for different angles of incidence θ.

	Individually -moored / Unmoored			**Inter-body moored / Unmoored**		
θ	0°	30°	60°	0°	0°	30°
$q_{\text{irr},1}$	0.954	0. 954	0. 955	0.964	0.964	0.965
$q_{\text{irr},2}$	0.954	0. 955	0. 955	0.966	0.965	0.965
$q_{\text{irr},3}$	0.954	0. 955	0. 955	0.966	0.963	0.965
Array	**0.954**	**0.955**	**0.955**	**0.965**	**0.964**	**0.965**

Table 1: Ratios of the time-averaged powers absorbed by the three-buoy array in irregular waves, for different configurations and values of the angle of incidence θ.

Fig. 8 shows that, as expected, the instantaneous values of the array dimensionless total power P^*_{irr} is significantly affected by the wave angle of incidence θ, although not its time-averaged value.

Table 1 shows the ratios between the time-averaged powers absorbed by the three buoys in the inter-body moored and in the individually-moored versus the unmoored configuration. It can be seen that, also for irregular waves, the inter-body moored configuration seems more favourable in terms of average power than the individually-moored configuration ($q^* > 1$).

5. Complex triangular-grid arrays

The equations derived before can be used without major difficulty to build up a mathematical model for more complex arrays consisting of buoys placed at the grid points of an equilateral triangular grid, with the weights located at the centres of the triangular cells. Each buoy is attached to 6 weights, if it is located inside the array, or to 1, 2, 3 or 4 weights if it is located at the periphery of the array. The array is spread-moored to the sea bed through its peripheric buoys, in such way that, in calm water, the whole assembly conforms to the specified pattern.

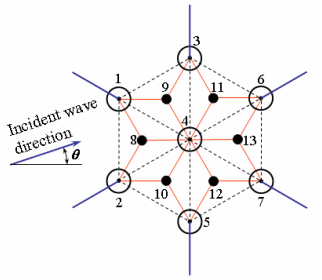

Figure 9: Seven-buoy array.

Results are presented in Figs. 10 and 11 for an array of seven (numbered 1 to 7) hemispherical point absorbers located at the vertices and the centre of a regular hexagon, and six (8 to 13) weights (Fig. 9). The numerical results are for regular waves of $A_w = 1$ m and $T = 10$ s, with $a = 7.5$ m, $H = 60$ m, $L_0 = 0.65 \times L_F$, $L_F = 60$ m, $L_R = 30$ m, $h = 35$ m, $W_F = W_R = 1520$ N/m and $C = 251.1$ kN/(m/s). In this scenario, in the static position, the bottom-mooring horizontal force at each buoy is balanced by connections to two weights, resulting in a body radius $a_8 = 0.63$ m and an inter-body mooring cable length $l_R = 48$ m.

Fig. 10 shows the surge and sway oscillations for the seven buoys, for an wave angle of incidence of $\theta = 0$. Due to symmetry, the results are identical (of opposite sign for sway) for pairs of buoys 1-2, 3-5, 6-7 (and also pairs of weights 9-10, 11-12), but not between different pairs due to different locations and mooring effects. It can be seen the nonlinear motions for the different buoys.

Fig. 11 shows again that the total absorbed power is significantly affected by wave angle of incidence ($\theta = 0$ and 30°) in terms of instantaneous values, but is almost insensitive in terms of time-averaged values. The smoothing effect on the array total power is visible.

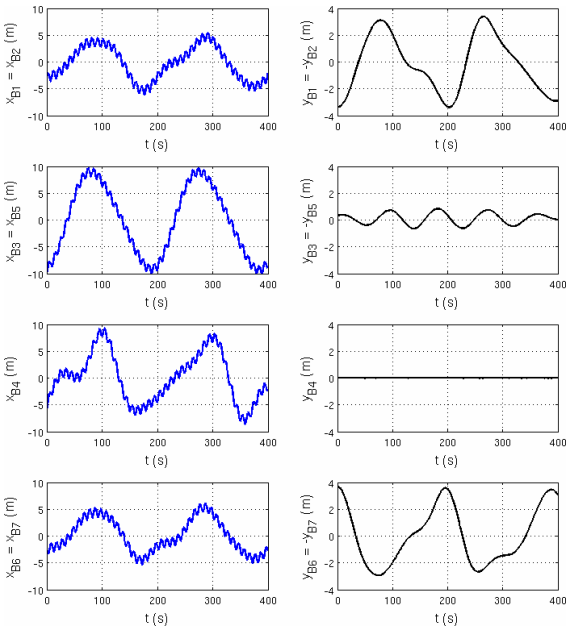

Figure 10: Surge and sway oscillations for the inter-body moored seven buoys. Regular waves of $A_w = 1\,\text{m}$, $T = 10\,\text{s}$.

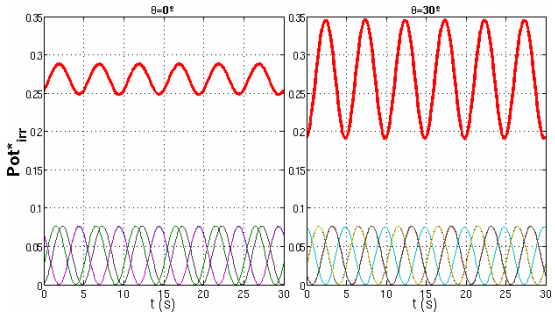

Figure 11: Instantaneous dimensionless power absorbed by the seven-buoy array with inter-body moorings (red solid line) and by each buoy of the array.

Conclusions

The results presented here illustrate the behaviour and power performance of triangular-grid arrays of identical wave energy converters, absorbing energy in the heaving mode from regular and irregular waves, spread-moored to the bottom through the bordering elements and inter-connected by lines kept under tension by weights.

The performance was found to be significantly affected by the presence of the mooring system.

A time-domain analysis was applied to investigate the nonlinear effects of the mooring forces in waves of moderate amplitude, effects that are not taken into account in the frequency domain analysis. The nonlinearities were found to affect much more markedly the horizontal oscillations: even in regular waves, they exhibit significantly non-simple-harmonic time-variations. This nonlinear behaviour derives from the nonlinear function of the cable tension and can be related to the system's natural oscillation frequency.

Acknowledgement

The work reported here was partly supported by the Portuguese Foundation for Science and Technology under contracts PTDC/EME-MFE/103524/2008, POCI-SFA-46 and PTDC/EME-MFE/66999/2006.

References

[1] M.E. McCormick. Ocean Wave Energy Conversion. Wiley, New York, 1981.

[2] I.J. Fylling. Anchoring systems for wave energy converters. Proc. 2nd Int. Symp. Wave Energy Utilization, Trondheim, Norway, 1982, p. 229-251.

[3] I. Johanning, G.H. Smith, J. Wolfram. Mooring design approach for wave energy converters. Proc. Inst. Mech. Eng. Part M-J. Eng. Marit. Environ., vol. 220, p. 159-174, 2006.

[4] L. Cleason, J. Forsberg, A. Rylander, B.O. Sjöström. Contribution to the theory and experience of energy production and transmission from the buoy-concept. Proc. 2nd Int. Symp. Wave Energy Utilization. Trondheim, Norway, 1982, p. 345-370.

[5] A. Weinstein, G. Fredrikson, M.J. Parks, K. Nielsen. Aquabuoy, the offshore wave energy converter numerical modelling and optimization. Proc. MTTS/IEEE Techno-Ocean '04 Conf., Kobe, Japan, 2004, vol. 4, p. 1854-1859.

[6] http://www.wavebob.com/

[7] http://www.oceanpowertechnologies.com/

[8] P. Ricci, J.-B. Saulnier, A.F. de O. Falcão. Point-absorber arrays: a configuration study off the Portuguese west coast. Proc. 7th European Wave Tidal Energy Conf., Porto, Portugal, 2007.

[9] P.C. Vicente, A.F. de O. Falcão, L.M.C. Gato, P.A.P. Justino. Hydrodynamics of multiple floating point-absorber wave energy systems with inter-body and bottom slack-mooring connections. Proc. 28th Int. Conf. Ocean Offshore Arctic Eng. OMAE 2009, Honolulu, Hawaii, 2009, Paper No. OMAE 2009-80245.

[10] J. Fitzgerald, L. Bergdahl. Including moorings in the assessment of a generic offshore wave energy converter: a frequency domain approach. Mar. Struct., vol. 21, p. 23-46, 2008.

[11] R.J. Smith, C.J. MacFarlane. Statics of a three component mooring line. Ocean Eng., vol. 28, p. 899-914, 2001.

[12] K. Ellermann. The Motion of floating systems: nonlinear dynamics in periodic and random waves. J. Offshore Mech. Arct. Eng. Trans. ASME, vol. 131, Paper 0411047, 2009.

[13] R. Pascoal, S. Huang, N. Barltrop, C.G. Soares. Assessment of the effect of mooring systems on the horizontal motions with an equivalent force to model. Ocean Eng., vol. 33, p. 1644-1668, 2006.

[14] W.E. Cummins. The impulse response function and ship motions. Schiffstechnik, vol. 9, p. 101-109, 1962.

[15] E.R. Jefferys. Device characterisation. In: Count B., editor, Power from Sea Waves. Academic Press, London, 1980, p. 413-438.

[16] J. Lighthill. An Informal Introduction to Theoretical Fluid Mechanics. Oxford University Press, Oxford, 1986.

[17] J. Falnes. Ocean Waves and Oscillating Systems. Cambridge University Press, Cambridge, 2002.

[18] Y. Goda. Random Seas and Design of Maritime Structures. 2nd edition, World Scientific, Singapore, 2002.